



**HAL**  
open science

## Sonochemical activity in ultrasonic reactors under heterogeneous conditions

A. Barchouchi, S. Molina-Boisseau, N. Gondrexon, Stéphane Baup

► **To cite this version:**

A. Barchouchi, S. Molina-Boisseau, N. Gondrexon, Stéphane Baup. Sonochemical activity in ultrasonic reactors under heterogeneous conditions. *Ultrasonics Sonochemistry*, 2021, 72, pp.105407. 10.1016/j.ultsonch.2020.105407 . hal-03119371

**HAL Id: hal-03119371**

**<https://hal.science/hal-03119371v1>**

Submitted on 16 Dec 2022

**HAL** is a multi-disciplinary open access archive for the deposit and dissemination of scientific research documents, whether they are published or not. The documents may come from teaching and research institutions in France or abroad, or from public or private research centers.

L'archive ouverte pluridisciplinaire **HAL**, est destinée au dépôt et à la diffusion de documents scientifiques de niveau recherche, publiés ou non, émanant des établissements d'enseignement et de recherche français ou étrangers, des laboratoires publics ou privés.



Distributed under a Creative Commons Attribution - NonCommercial 4.0 International License

# Sonochemical activity in ultrasonic reactors under heterogeneous conditions

Barchouchi A.<sup>1</sup>, Molina Boisseau S.<sup>2</sup>, Gondrexon N.<sup>1</sup>, Baup S.<sup>1,\*</sup>

<sup>1</sup>Univ. Grenoble Alpes, CNRS, Grenoble INP, LRP, 38000 Grenoble, France

<sup>2</sup>Univ. Grenoble Alpes, CNRS, CERMAV, 38000 Grenoble, France

## Abstract

Due to its physical and chemical effects, ultrasound is widely used for industrial purposes, especially in heterogeneous medium. Nevertheless, this heterogeneity can influence the ultrasonic activity. In this study, the effect of the addition of inert glass beads on the sonochemical activity inside an ultrasonic reactor is investigated by monitoring the formation rate of triiodide, and the ultrasonic power is measured by calorimetry and by acoustic radiation. It was found that the sonochemical activity strongly depends on the surface area of the ~~surface developed by the~~ glass beads in the medium: it decreases above a critical area value (around  $10^{-2}$  m<sup>2</sup>), partly due to wave scattering and attenuation. This result is confirmed for a large range of frequencies (from 20 to 1135 kHz) and glass beads diameters ~~glass beads~~ (from 8-12  $\mu$ m to 6 mm). It was also demonstrated that above a given threshold of the ~~developed surface~~ area, only part of the supplied ultrasonic power is devoted to chemical effects of ultrasound. Finally, the acoustic radiation power appears to describe the influence of solids on sonochemical activity, contrary to the calorimetric power.

## Highlights

- Ultrasonic power measured by calorimetry is not affected by glass beads addition
- Glass beads surface area is a relevant criterion to describe sonochemical activity
- Sonochemical activity decreases above a critical surface area for all frequencies
- Acoustic radiation power is relevant to describe glass beads effect on sonoactivity

Keywords: Ultrasound; Sonochemistry; Calorimetry; Acoustic radiation power; Heterogeneous media; Suspension

## 1. Introduction

Many applications are reported about low and high frequency ultrasound, applied in various sonochemical processes involving heterogeneous media. For example, nanostructured materials can be synthesized at ambient temperature and pressure, in a short reaction time, with the use of power ultrasound. It is even possible to control the size of powder and/or modify the material surface [1,2]. Ultrasound can also be used to enhance solid-liquid extraction: this ultrasound-assisted extraction allows to recover heat-sensitive bioactive

39 compounds at low temperature and promote the use of GRAS (generally recognized as safe)  
40 solvent [3]. Also in adsorption process, the regeneration of the adsorbent and the mass transfer  
41 were proven to be improved by means of ultrasonic waves [4]. Another example is  
42 sonocrystallisation, where ultrasound is used to decrease the induction time and the  
43 metastable zone, and to increase the nucleation rate. Crystals with controlled size and  
44 distribution are likely to be obtained [5].

45 Even if ultrasound in heterogeneous medium is widely used in such different domains, only  
46 few articles are dedicated to the study on the influence of heterogeneity on the sonochemical  
47 activity. Main studies previously reported are summarized in **Table 1**, where the surface area  
48 of the particles is calculated according to the data available in these papers. In 2002, Keck *et*  
49 *al.* investigated the influence of quartz particles (2 - 25  $\mu\text{m}$ ) on the chemical effects induced  
50 by ultrasound from 68 to 1028 kHz, under Ar/O<sub>2</sub> or N<sub>2</sub>/O<sub>2</sub> conditions. The authors noticed the  
51 activity increases at 206 kHz due to a bubbles shape modification, which enables more  
52 radicals release in the bulk by increasing bubble interface [6]. They also reported that the  
53 ultrasonic activity was reduced for all the other frequencies, due to ultrasound attenuation.  
54 Tuziuti *et al.* (2005) studied the enhancement of sonochemical reaction by adding different  
55 amounts (0 - 100 mg) of alumina particles (1 - 80  $\mu\text{m}$ ). They observed that with an  
56 appropriate amount (20 mg) and size (20  $\mu\text{m}$ ) of particles, the sonochemical activity increases  
57 by increasing the population of cavitating bubbles [7]. Her *et al.* (2011) investigated the role  
58 of inert or TiO<sub>2</sub> coated glass beads (from 50 to 5000  $\mu\text{m}$  diameters) on the H<sub>2</sub>O<sub>2</sub> production.  
59 Their conclusion was that the inert glass addition increases the sonochemical activity at low  
60 frequency (28 kHz) by increasing the formation rate of cavitation bubbles. At higher  
61 frequencies (580 and 1000 kHz) this activity decreases, except for 100  $\mu\text{m}$  (10-50 g.L<sup>-1</sup>), due  
62 to wave-particle interference [8]. Stoian *et al.* (2018) studied the influence of particle addition  
63 (ion exchange resin, sand, and glass beads) with different diameters (207 - 1290  $\mu\text{m}$ ) and  
64 concentrations on the sonochemical activity in a full stirred reactor at 20 kHz. The authors  
65 found that the sonochemical activity of ultrasound is changed according to the particle  
66 concentration. They reported a first decrease due to wave attenuation, for volumetric solid  
67 concentrations (C<sub>v</sub>) from 0 to 0.01. Then they reported an increase of the sonochemical  
68 activity for C<sub>v</sub> from 0.01 to 0.4, due to the enhancement of cavitation bubbles. However,  
69 above C<sub>v</sub> = 0.4, this activity decreased due to change of the medium viscosity [9]. More  
70 recently, Son *et al.* (2019) have investigated the cavitation activity in heterogeneous systems  
71 containing fine particles in a 28 kHz double-bath sonoreactor. Their results clearly suggested  
72 that there were no significant differences in calorimetric energies for both with and without  
73 particles conditions. Furthermore, the chemical activity was evaluated using  
74 sonochemiluminescence (SCL) and different trends were observed depending on the presence  
75 and size of beads [10].

76 In order to obtain complementary understanding on the effect of heterogeneity on ultrasound  
77 activity, this research aims to investigate the influence of the presence of divided solids on  
78 sonochemical activity within a low or high frequency ultrasonic reactor. Inert glass beads are  
79 used in order to simulate solid heterogeneity, with different diameter and concentration.  
80 Diameters were chosen considering the characteristic parameters of an ultrasonic system: its  
81 wavelength and the diameter of its acoustic cavitation bubbles. The global ultrasonic activity

82 and the chemical ultrasonic activity were quantified by different methods and they were  
 83 systematically compared in homogeneous and heterogeneous conditions. The ultrasonic  
 84 power was measured by calorimetry while the chemical activity was monitored by iodide  
 85 dosimetry.

86 **Table 1. Summary of main publications about ultrasound in heterogeneous media**

Authors	Particles	Diameter (µm)	Concentration (g.L <sup>-1</sup> )	Calculated area (m <sup>2</sup> )	Frequency (kHz)	Gas condition	Reported effects
Keck et al. [6]	Quartz	2-25	1-25	0.15-10 <sup>4</sup>	68-206-353-620-1028	N <sub>2</sub> /O <sub>2</sub> Ar/O <sub>2</sub>	The particle addition reduces the sonochemical activity except at 206 kHz
Lu et al. [11]	Silica Alumina	2-130 130	2-200	0.92-6 10 <sup>3</sup>	20	Air	The sonoactivity is reduced, for all diameters and concentrations
Tuziuti et al. [7]	Alumina	1-80	10-100	0.38-15.2	42	Air	The sonoactivity is increased with an appropriate particle size and concentration
Her et al. [8]	Glass with and without TiO <sub>2</sub> coating	50-5000	10-200	48-4800	28-580-1000	Air	The sonoactivity is decreased with particle addition except at 28 kHz
Stoian et al. [9]	Resin Sand Glass	625 309 207-1290	12.2-610	12.2-30.2	20	Air	The sonoactivity is maximal for a 0.4 solid volumetric concentration
Son et al. [10]	Clay Glass	75 75-2000	100-333	0.12-3.2	28	Air	No difference in calorimetric energies. SCL depends on the presence and the size
This research	Glass beads	8-6000	0.003-80	1.5 10 <sup>-4</sup> -0.95	20-376-575-858-1135	Air Ar	

87

## 88 2. Materials and methods

### 89 2.1 . Ultrasonic reactors

90 Two different devices are used to generate ultrasound. The high frequency generator MFG  
 91 and the corresponding transducers are provided by Meinhardt Ultrasonics (**Fig 1.a**). Two  
 92 transducers are used in order to vary frequency: 376, 575, 858 and 1135 kHz are studied.  
 93 These interchangeable flat transducers (50 mm diameter) are placed at the bottom of the  
 94 vessel. The low frequency equipment is a homemade cup horn based on a 20 kHz Sonics  
 95 Vibracell 75115 generator (**Fig 1.b**) with a 25 mm probe.

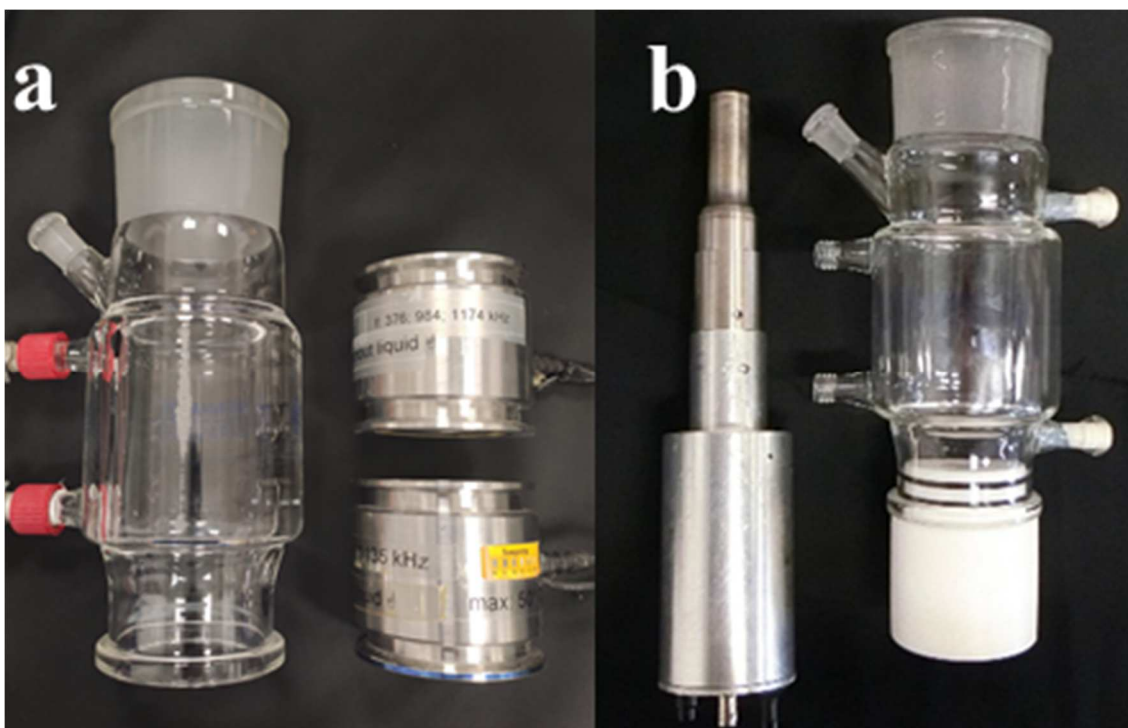


Fig. 1. Ultrasonic reactors (1.a: high frequency reactor, 1.b: low frequency reactor)

96  
97

98 For both devices, the same 500 mL reactor vessel is used, with a double jacket in order to  
99 maintain a constant temperature at  $20 \pm 1$  °C, thanks to a cryothermostat bath (Thermo Fisher  
100 Scientific Arctic A25). Each experiment last 30 minutes, and triplicates are carried on. As the  
101 used vessels are very similar, the reactor shape is not likely to influence the obtained results  
102 [12,13].

### 103 2.2 Glass beads

104 In order to simulate the heterogeneity in the medium, glass beads are used. They were chosen  
105 because they are easy to characterize through their diameter and chemically inert. Preliminary  
106 tests have shown triiodide adsorption is negligible (less than 1%) and SEM photographs have  
107 proven sonication has no effect on beads structure. These beads were used at different mass  
108 concentrations, ranging from  $3.2 \cdot 10^{-3}$  to  $80 \text{ g.L}^{-1}$ .

109 A wide range of glass beads diameters (between 8-12 and  $6000 \mu\text{m}$ ) was tested. The objective  
110 was to be in the same order of magnitude as the wavelength (from 1400 to  $4000 \mu\text{m}$  for high  
111 frequency) and the cavitation bubbles diameter. From 213 to 1136 kHz, the cavitation bubbles  
112 diameter was estimated to be from 4 to  $8 \mu\text{m}$  thanks to the work of Brotchie et al. [14], and it  
113 was also calculated from 2.8 (at 1174 kHz) to  $164.5 \mu\text{m}$  (at 20 kHz) with Minnaert equation  
114 [15].

### 115 2.3 Calorimetry

116 The ultrasonic power ( $P_{US}$ ) supplied to the medium was measured by calorimetry [16]. This  
117 method is classically used to thermally characterize an ultrasound device by monitoring the  
118 temperature change of the irradiated medium. Carefully The reactor is thermally insulated  
119 carefully by glass wool, and two temperature probes are placed within the reactor to confirm  
120 the temperature homogeneity inside the irradiated medium. Before calorimetry, the

121 temperature of the liquid inside the vessel is reduced by 5°C under the ambient temperature,  
122 and the monitoring stops when the temperature of the irradiated liquid is 5°C above the  
123 ambient temperature.

124 Assuming that the reactor is thermally insulated, the ultrasonic power is obtained by the  
125 following energy balance:

$$126 \quad P_{US} = m_{\text{water}} C_{p,\text{water}} \frac{dT}{dt} \quad (1)$$

127 where  $m_{\text{water}}$  is the mass of water contained in the reactor (0.5 kg),  $C_{p,\text{water}}$  is the heat capacity  
128 of water (4.18 kJ.kg<sup>-1</sup>.K<sup>-1</sup>) and  $\frac{dT}{dt}$  is the slope of the experimental curve at the point where the  
129 temperature of the sonicated water equals the ambient temperature.

130 Nevertheless, the obtained value gives the net ultrasonic power ~~present~~ dissipated in the  
131 medium. The ultrasonic power absorbed by the reactor vessel must be estimated. So a  
132 calibrated resistance (11.5 Ohm) is used with a power supply (Française d'Instrumentation FI  
133 3610) at 2.97 A and 34 V in order to measure the energy absorbed by the vessel. This energy  
134 is turned into an equivalent mass of water to be added at the energy balance as follows:

$$135 \quad P_{US} = (m_{\text{water}} + m_{\text{eq-water}}) C_{p\text{Water}} \frac{dT}{dt} \quad (2)$$

136 where  $m_{\text{eq-water}}$  is the energy absorbed by the ~~reactor~~ vessel converted into an equivalent mass  
137 of water. Finally, the total ultrasonic power ~~generated~~ transferred by the transducer is  
138 calculated by equation (2).

## 139 **2.4 KI dosimetry**

140 Considered as reproductive, easy to set up and reliable [17], this technique is based on the  
141 irradiation of an aqueous solution of potassium iodide (KI) by ultrasound [18]. A fraction of  
142 iodide (I<sup>-</sup>) is oxidized into diiodine (I<sub>2</sub>) by radicals produced by cavitation bubbles implosion.  
143 Then the rest of iodine reacts with diiodine. So the final product triiodide (I<sub>3</sub><sup>-</sup>) is generated  
144 according to the following reaction:



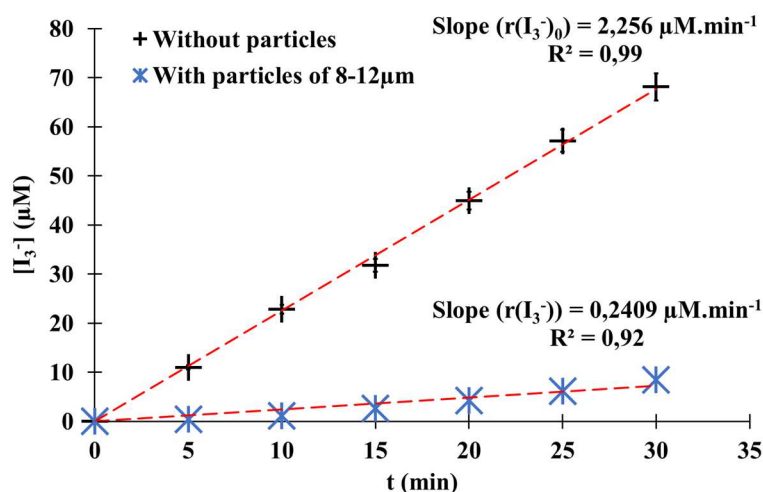
146 From an initial solution of potassium iodide (10 g.L<sup>-1</sup>), the absorbance of the yellow triiodide  
147 is measured at 355 nm (spectrophotometer Shimadzu UVmini 1240). Finally, its  
148 concentration is obtained thanks to its molar attenuation coefficient ( $\epsilon = 26300 \text{ L.mol}^{-1}.\text{cm}^{-1}$ ).

149 For heterogeneous medium, addition of glass beads was considered since the obtained  
150 solution is homogenized even for the highest concentration. Therefore, hydrodynamic  
151 conditions are thereby nearly the same than under homogeneous conditions and the ultrasonic  
152 reactor can be considered as a batch reactor. So, the following equation is obtained thanks to  
153 the mass-balance based on triiodide production and provides the triiodine formation rate  $r(\text{I}_3^{-})$ :

$$154 \quad r(\text{I}_3^{-}) = \frac{1}{V} \cdot \frac{dn_{\text{I}_3^{-}}}{dt} = \frac{\Delta[\text{I}_3^{-}]}{\Delta t} \quad (4)$$

155 Moreover the concentration of triiodide increases linearly with sonication time (**Fig. 2**).  
156 Assuming the triiodide formation reaction follows a zero-order kinetics, triiodide formation

157 rate is likely to be directly estimated by the value of the slope of the obtained straight line, as  
 158 proposed by [19].



159  
 160 Fig. 2. Examples of chemical characterization by iodometry of an ultrasonic system at 575 kHz  
 161 ( $d_p = 8-12 \mu\text{m}$ ,  $V = 500 \text{ mL}$ ,  $P_{US} = 51.5 \pm 0,5 \text{ W}$ ,  $T = 20 \pm 1 \text{ }^\circ\text{C}$ )

162 ~~In this study, two types of triiodide formation rate are defined.~~ In this study, we defined two  
 163 different notations for triiodide formation rate: in the case of homogeneous media (without  
 164 particles) the formation rate is represented by  $r(I_3^-)_0$  whereas in the case of heterogeneous  
 165 media (presence of glass beads) the formation rate is denoted  $r(I_3^-)$ .

## 166 2.5 Acoustic radiation power

167 When a solid target is immersed in a liquid irradiated by ultrasound, it undergoes a radiation  
 168 force providing some information about the acoustic radiation power [20], denoted  $P_{US-rad}$ .  
 169 This power is measured according to the International Electrotechnical Commission (IEC)  
 170 61161 norm [21]: a silicon target (diameter 6.5 cm) is set at the liquid surface and hooked to a  
 171 precision balance (Kern-PCB 2500-2) in order to record its weight. Then the acoustic  
 172 radiation power is calculated by the following equation

$$173 P_{US-rad} = \Delta m \cdot g \cdot c \quad (5)$$

174 where  $g$  is the gravitational acceleration ( $9.81 \text{ m}\cdot\text{s}^{-2}$ ),  $\Delta m$  is the difference of weight with and  
 175 without ultrasound (kg), and  $c$  is the sound velocity in water ( $1500 \text{ m}\cdot\text{s}^{-1}$ ).

176 The acoustic radiation power depends on several parameters of the target (material, size,  
 177 distance from the transducer ...) [22-23] but the obtained values are in the same range as the  
 178 power obtained by calorimetry, according to the literature [24-26]. In our case, experiments  
 179 were only performed at 575 kHz, because target is damaged for higher frequencies.

## 180 2.6 Gas experiments

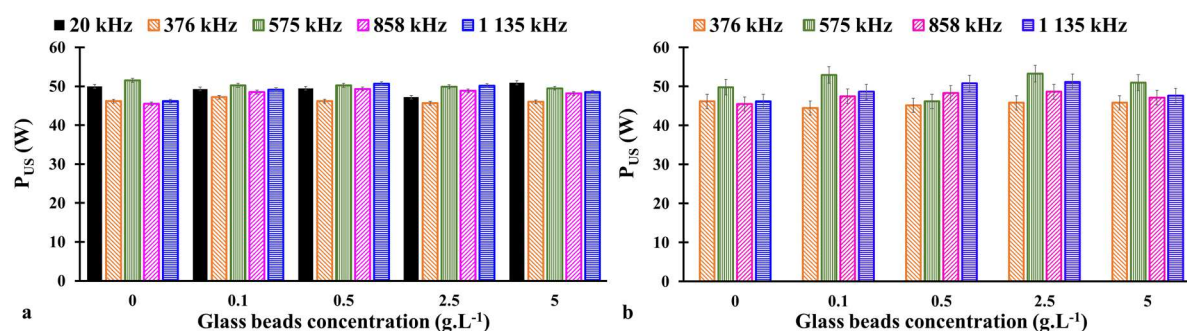
181 Most of experiments are achieved with an atmospheric open vessel, under air conditions, but  
 182 sonochemical activity is influenced by dissolved gases. As a consequence, some experiments  
 183 are carried on under argon. For these trials, water is preliminary deaerated and saturated by  
 184 argon bubbling for 20 minutes. Then the sonication is performed with a slight argon current  
 185 maintained just above the liquid surface, to avoid any oxygen and nitrogen dissolution.

## 186 3. Results and discussion

### 187 3.1. Ultrasonic power measured by calorimetry: effect of particles

188 In order to investigate the effect of heterogeneous media on  $P_{US}$ , calorimetric experiments  
189 were carried out first without heterogeneity (ultra-pure water), then in the presence of glass  
190 beads, with different diameters and different concentrations.

191 In a homogeneous medium ( $0 \text{ g.L}^{-1}$ ), the electrical input power was adjusted to obtain a  
192 similar ultrasonic power (around 50 W) for all the studied frequencies as shown in Fig 3.a.



193 Fig. 3. Ultrasonic power measured by calorimetry. a: with 8-12  $\mu\text{m}$  glass beads, b: with 90-150  $\mu\text{m}$  glass beads

195 ~~For the studied frequencies and~~ Then, at the same electrical power level, for all the studied  
196 frequencies and in presence of 8-12  $\mu\text{m}$  diameter glass beads, the ultrasonic power was  
197 measured by calorimetry. ~~in heterogeneous medium was represented in~~ The result is displayed  
198 in Fig. 3.a. It can be observed that the addition of particles has no effect on  $P_{US}$  whatever the  
199 concentration is in the range from 0.1 to 5  $\text{g.L}^{-1}$ , because the obtained calorimetric power is  
200 close to 50 W for all the concentrations. This result was corroborated by other glass bead  
201 diameters (Fig 3.b). Moreover, some complementary experiments were carried out for the 5  
202 frequencies with an ultrasonic power of 22 W and the addition of particles has also no effect  
203 on  $P_{US}$ .

204 All these observations put in evidence that the ultrasonic power measured by calorimetry is  
205 not influenced by the presence of glass beads. The same result was observed by Stoian et al.  
206 in terms of volumetric power [9]. The dissipated power ~~global energy available~~ in the system  
207 remains unchanged for all our experimental operating conditions. While such an observation  
208 is in good agreement with recent work by Son et al. [10], it is expected that complementary  
209 data dealing with the sonochemical activity should give more information.

### 210 3.2. Ultrasonic chemical activity measured by iodometry: effect of particles 211 addition

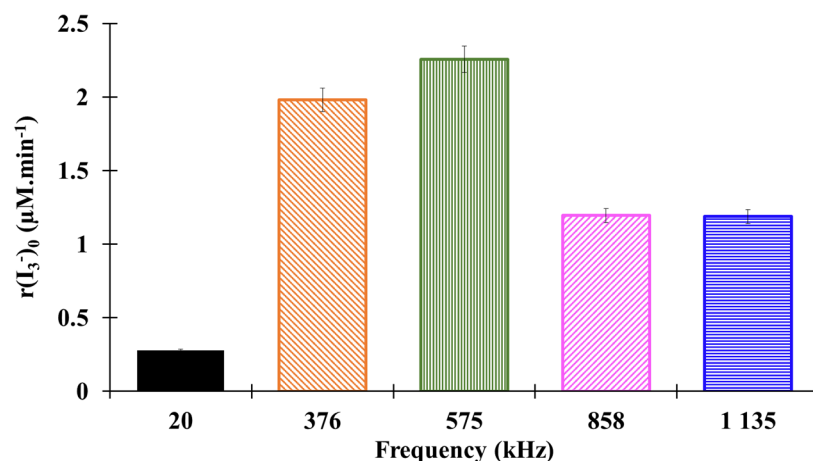
212 The sonochemical activity was monitored by potassium iodide dosimetry and the formation  
213 rate  $r(\text{I}_3^-)$  is a relevant indicator of the amount of radical species produced by sonolysis of  
214 water [27].

#### 215 3.2.1. Sonochemical activity in homogenous media

216 For all the experiments, the reactors have the same shape and volume, and the same ultrasonic  
217 power is adjusted. So the frequency is assumed to be the single parameter likely to influence  
218 the sonochemical activity. The triiodide formation rates ( $r(\text{I}_3^-)_0$ ) are plotted according to the  
219 frequencies (Fig 4). As it can be seen, results show a maximal rate at 575 kHz with a value of  
220  $2.3 \pm 0.1 \mu\text{M.min}^{-1}$ , and a minimal rate at low frequency with a value of  $0.28 \pm 0.01 \mu\text{M.min}^{-1}$



221 <sup>1</sup>. So, the optimal sonochemical activity is obtained at 575 kHz and the sonochemical activity  
222 is ~~divided by a factor of 10~~ ten-fold lower at 20 kHz. This result is in accordance with the  
223 literature: the same ~~decreasing factor~~ ratio between high and low frequencies was reported by  
224 Koda [18].

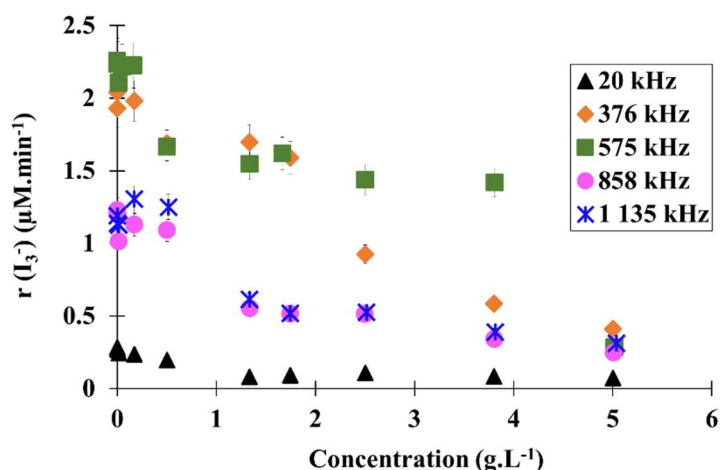


225  
226 **Fig. 4. Sonochemical activity measured by iodometry in homogeneous medium (V = 500 mL, P<sub>US</sub> = 51.5 ± 0.5 W)**

227 The maximal sonochemical activity between 300 and 600 kHz was previously reported by  
228 different authors [18, 28-30] and was explained by a larger population of active cavitation  
229 bubbles when the frequency increases. But this beneficial effect of the frequency is reduced  
230 for higher frequencies by the reduction of the growth time of cavitation bubbles, which leads  
231 to a reduction of sonochemical activity [31]. Therefore, our study mainly focused on the  
232 sonochemical activity at high frequency, and most of the results reported in this paper were  
233 obtained at 575 kHz.

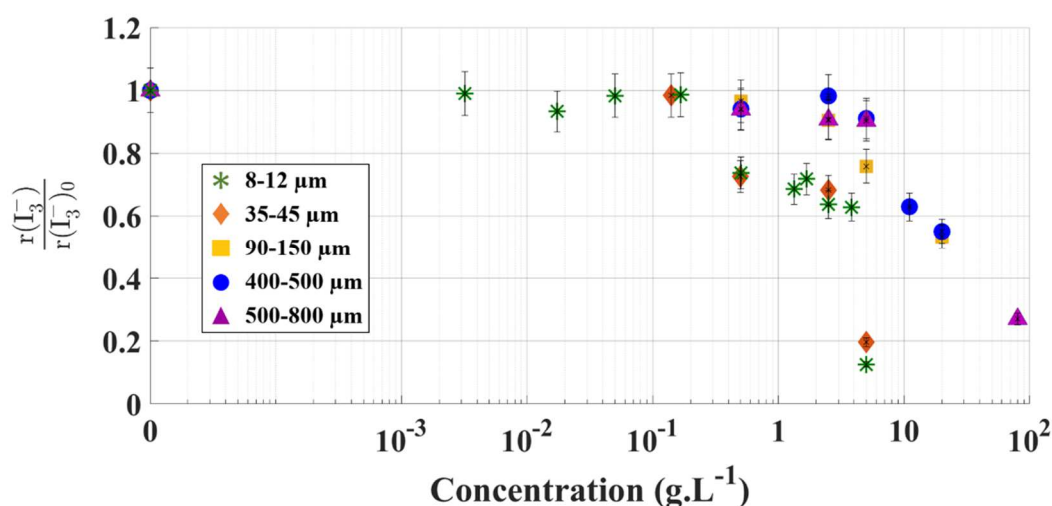
### 234 **3.2.2. Sonochemical activity in heterogeneous media**

235 In order to investigate if the sonochemical activity is affected by solid heterogeneity, the rates  
236 of triiodide formation (r(I<sub>3</sub><sup>-</sup>)) in the presence of glass beads were measured as previously  
237 detailed in this paper (**Fig. 2**). Experimental formation rates observed with 8-12 μm diameter  
238 glass beads are given in **Fig 5**. First of all, results exhibit that 575 kHz is the most efficient  
239 frequency for all the glass beads concentrations, as in homogeneous media. Secondly  
240 whatever the frequency is, it can be noticed that r(I<sub>3</sub><sup>-</sup>) decreases when the particles  
241 concentration increases. In the literature, this result is controversial because on the one hand  
242 the particle addition may promote the acoustic cavitation by reducing the cavitation threshold  
243 and may increase the number of nucleation sites or even modify the shape of imploding  
244 bubbles releasing more radicals [6,12]. On the other hand, at more concentrated media, the  
245 acoustic cavitation may decrease because of the wave attenuation [6-8].



246  
247  
248 Fig. 5. Effect of glass bead concentration on triiodide formation rate, for different frequencies  
( $d_p = 8-12 \mu\text{m}$ ,  $V = 500 \text{ mL}$ ,  $P_{US} = 51.5 \pm 0,5 \text{ W}$ ,  $T = 20 \pm 1 \text{ }^\circ\text{C}$ )

249 Similar experiments were then performed with other glass beads diameters. To highlight the  
250 influence of these glass beads, results are presented using a ratio defined as the rate of  
251 triiodide formation in heterogeneous medium ( $r(I_3^-)$ ) divided by the formation rate in  
252 homogeneous medium ( $r(I_3^-)_0$ ). As shown in **Fig. 6** at low glass beads concentration,  $I_3^-$   
253 formation rates ratio remains constant and close to 1, illustrating the sonochemical activity is  
254 not affected by the presence of particles, whatever the glass beads diameter. To our  
255 knowledge, this phenomenon has never been reported in the literature [6-9]. According to  
256 experimental results exhibited in **Fig. 6**, it seems that for each glass beads diameter, the  $I_3^-$   
257 formation rates ratio decreases above a certain particle concentration, ~~partially due to wave~~  
258 ~~attenuation.~~



259  
260  
261 Fig. 6. Effect of the glass bead concentration on the triiodide formation rate, for different diameters  
( $f = 575 \text{ kHz}$ ,  $V = 500 \text{ mL}$ ,  $P_{US} = 51.5 \pm 0.5 \text{ W}$ ,  $T = 20 \pm 1 \text{ }^\circ\text{C}$ )

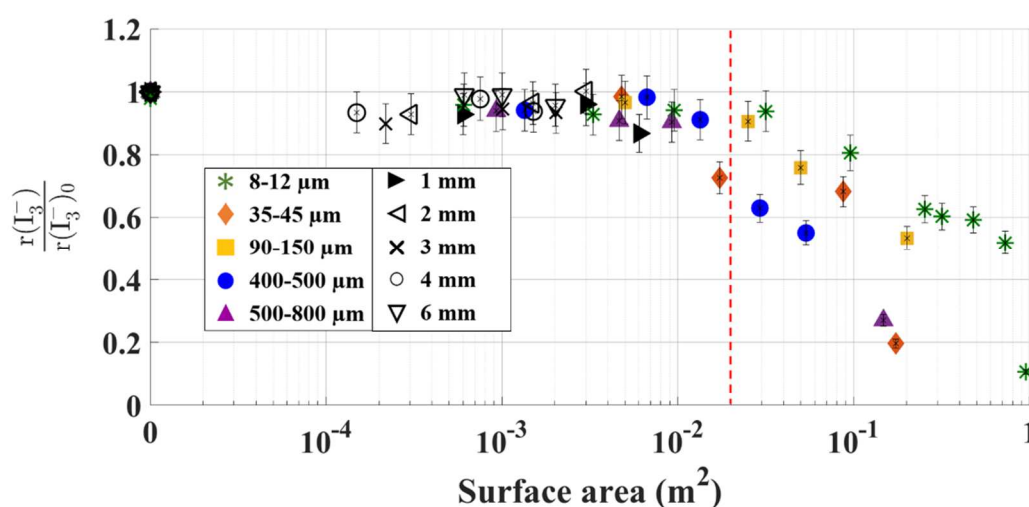
262 For all these experiments, both diameter and concentration of particles are likely to be  
263 ~~different~~. So, in order to take into account these two parameters simultaneously, the area of  
264 the ~~developed~~ surface due to the presence of beads inside the reactor was considered as a new  
265 criterion to express the results. It is defined as the area of the surface induced by the amount

266 of glass beads introduced within the reactor, and it is calculated thanks to the following  
 267 equation.

268 
$$\text{Surface area: } A = \frac{6}{\rho_{\text{glass}} d_p} m_p \quad (6)$$

269 with  $m_p$ : total mass of particles,  $d_p$ : mean particle diameter and  $\rho_{\text{glass}} = 2500 \text{ kg}\cdot\text{m}^{-3}$ .

270 Results obtained at 575 kHz are exhibited on **Fig. 7**. Whatever the particles diameter is, the  $I_3^-$   
 271 formation rates ratio is close to 1 at low developed surface area value. It means the ultrasonic  
 272 activity is not influenced by the particles addition. Nevertheless, chemical effect of ultrasound  
 273 decreases sharply above a typical value of the surface area. This critical value was found to be  
 274 between  $10^{-2}$  and  $3\cdot 10^{-2} \text{ m}^2$ , varying according to the bead size.



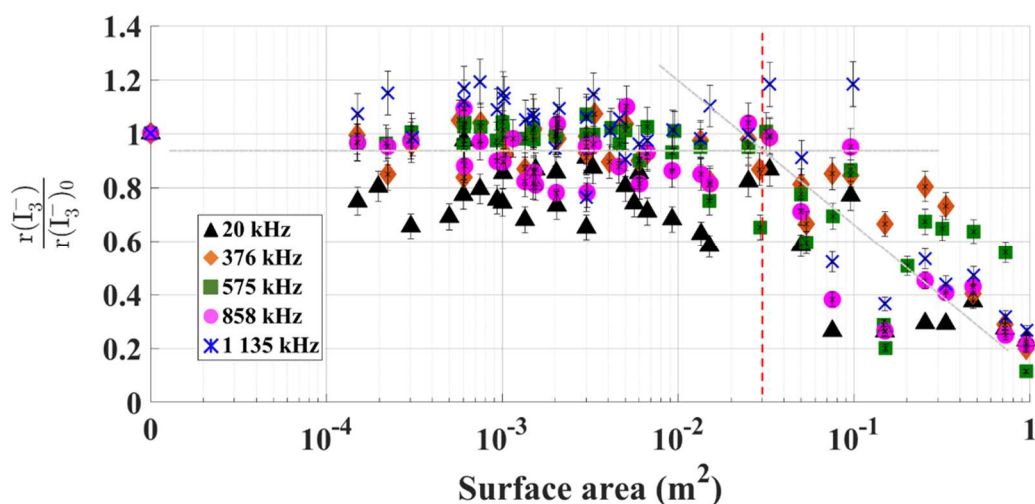
275  
 276 **Fig. 7. Normalized  $I_3^-$  formation rates, for different surface areas and diameters.**  
 277 ( $f = 575 \text{ kHz}$ ,  $V = 500 \text{ mL}$ ,  $P_{\text{US}} = 51.5 \pm 0.5 \text{ W}$ ,  $T = 20 \pm 1 \text{ }^\circ\text{C}$ )

278 According to the literature, the effect of inert particles on sonochemical activity is considered  
 279 to result from two types of interaction. The first interaction takes place between the waves and  
 280 the particles, and it provokes an attenuation and a scattering of the ultrasonic waves for  
 281 concentrated suspensions [6-9] (Table 1). The second interaction takes place between the  
 282 particles and the cavitation bubbles: the particles can interfere at the different stages of the  
 283 cavitation bubble lifetime. (i) At the initial nucleation step, the solid particles can be supposed  
 284 to act as additional nucleation sites [32], so their presence will improve the sonochemical  
 285 activity by increasing the number of bubbles. (ii) At the growing stage, it was reported that  
 286 small and low-density particles can be located at the ultrasonic wave antinodes where the tiny  
 287 bubbles grow and become active resulting in a detrimental competition [33]. (iii) At the last  
 288 phase of the cavitation bubble lifetime, the presence of particles is generally supposed to  
 289 promote asymmetric implosions enhancing thereby the sonochemical activity [6-8].

290 In our case, below the critical area, the sonochemical activity remains unchanged. On the one  
 291 hand, this is due to the fact that the particles did not play the role of nucleation site, because  
 292 the used glass beads are smooth and not small enough, which can reduce the probability of the  
 293 cavitation occurrence according to the work of Zhang et al. [34]. On the other hand, there is

294 no wave scattering and attenuation due to the low particle concentration. Furthermore, no  
 295 second interaction can be expected at this level because the glass beads are too dense to be  
 296 trapped at the wave antinodes. Nevertheless, as they can be dragged away by the acoustic  
 297 streaming, the particles did not play the role of solid wall, which enhance radical release by  
 298 modifying the shape of imploding bubbles as described by Keck [6] or Tuziuti [7].

299 However, above the critical area value, the sonochemical activity is dramatically decreased,  
 300 that cannot be only due to the wave scattering and attenuation ~~like it was~~ as reported in the  
 301 literature [6-9,11], because our highest particle concentration (80 g.L<sup>-1</sup>) is lower than the  
 302 concentrations used by these researchers (Table 1). For example, Stoian [9] worked with a  
 303 concentration between 12.2 g.L<sup>-1</sup> and 610 g.L<sup>-1</sup> and Tuziuti [7] used a concentration from 10  
 304 to 100 g.L<sup>-1</sup>. Finally, it can be thought that the particles may induce an asymmetric implosion,  
 305 likely to decrease sonochemical activity, according to different studies [11, 35].

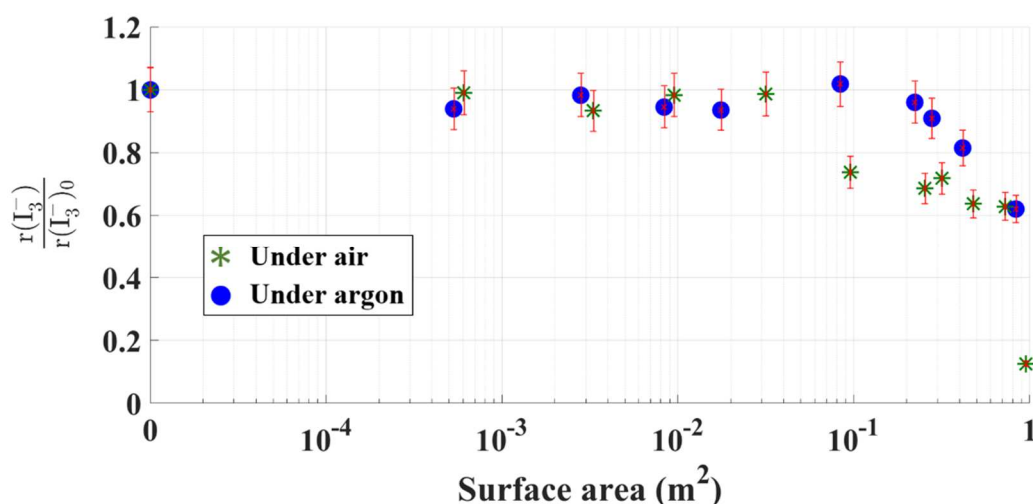


306  
 307 **Fig. 8. I<sub>3</sub><sup>-</sup> formation rates ratio at different frequencies for different surface areas and diameters.**  
 308 (V = 500 mL, P<sub>US</sub> = 51.5 ± 0.5 W, T = 20 ± 1 °C, d<sub>p</sub> from 8-12 μm to 6 mm)

309 As surprisingly shown in **Fig. 8**, the same trend was observed for all the ultrasonic  
 310 frequencies used in this work: the sonochemical activity first remains unchanged and then  
 311 sharply decreases above the same critical surface area inside the reactor. So, for these studied  
 312 frequencies, the addition of inert glass particles reduces the sonochemical activity above a  
 313 critical area, estimated to be 3.10<sup>-2</sup> m<sup>2</sup>.

### 314 3.2.3. Effect of gas on sonochemical activity in heterogeneous media

315 As for a homogeneous medium, sonochemical activity in a heterogeneous medium is  
 316 influenced by dissolved gases. According to the gases, oxidant species are not the same, so  
 317 chemical reactions pathways are modified. For instance, sonication of water under air leads to  
 318 the formation of different species, among which nitrites and nitrates whereas sonication under  
 319 argon is known to be •OH specific [36]. So experiments were carried on under argon  
 320 conditions (section 2.6) with and without 8-12 μm glass beads, with a 51.5 ± 0.5 W  
 321 calorimetric power at 575 kHz.



322  
323 **Fig. 9. Combined effect of gas and glass beads presence on triiodine formation rate**  
324 ( $d_p = 8\text{-}12 \mu\text{m}$ ,  $f = 575 \text{ kHz}$ ,  $V = 500 \text{ mL}$ ,  $P_{US} = 51.5 \pm 0.5 \text{ W}$ ,  $T = 20 \pm 1 \text{ }^\circ\text{C}$ )

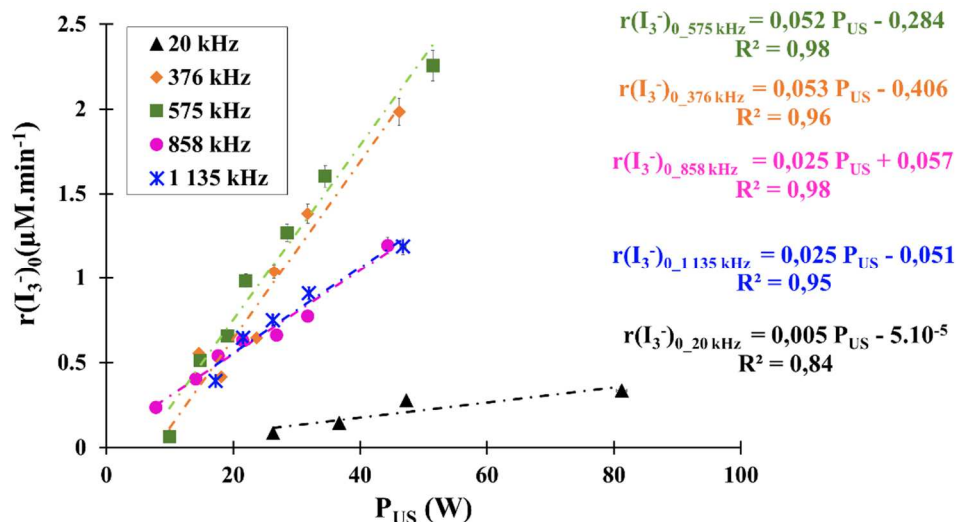
325 Without any beads, triiodine formation rate decreases from  $2.3 \pm 0.1 \mu\text{mol}\cdot\text{min}^{-1}$  under air  
326 condition to  $0.65 \pm 0.04 \mu\text{mol}\cdot\text{min}^{-1}$  under argon condition. Under argon condition, there is no  
327 contribution of the oxidant reagents generated by oxygen ( $\bullet\text{OOH}$ ,  $\bullet\text{OH}$  et  $\text{O}$ ) as reported in the  
328 literature [37-42], so the triiodine formation rate declines.

329 In the presence of glass beads, results obtained under air and argon conditions were compared  
330 (Fig. 9). Both curves exhibit the same trend: a first plateau where the sonochemical activity  
331 remains constant followed by a drastic decrease above a critical value of the developed  
332 surface area. As previously explained, this reduction of activity is probably due to wave  
333 attenuation and to less energetic bubbles implosions [35, 43-45]. Under argon conditions, the  
334 value of the critical developed surface area (close to  $3 \cdot 10^{-1} \text{ m}^2$ ) is higher than the value  
335 observed for air conditions (close to  $3 \cdot 10^{-2} \text{ m}^2$ ). For argon, even if the sonochemical activity is  
336 initially lower, its decrease appears to be less important. It can be explained by the higher  
337 temperature reached when cavitation bubbles implode, due to this mono-atomic gas presence  
338 inside these bubbles [26, 46-49] that counteracts the detrimental effect of glass beads.

339 Even if iodometry under argon condition is much more  $\bullet\text{OH}$  specific compared to air  
340 condition, the same trend is obtained for both conditions. So air iodometry is likely to be used  
341 to describe the effect of glass beads addition within an ultrasound reactor.

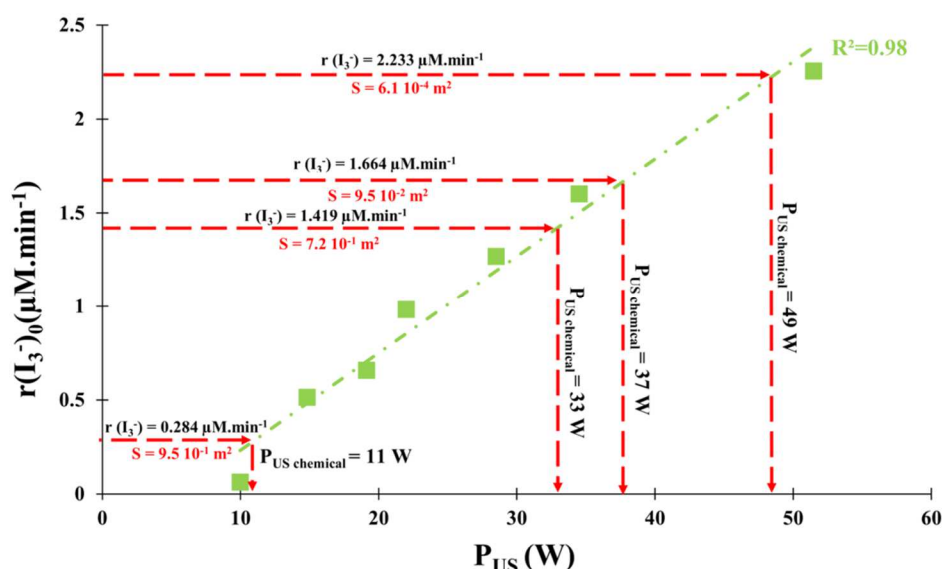
### 342 3.3. The real ultrasonic power devoted to sonochemistry

343 Whatever the frequency is, for all the beads diameters and concentrations, the calorimetric  
344 ultrasonic power ( $P_{US}$ ) released inside the reactor in heterogeneous medium was constant  
345 (section 3.1) while the sonochemical activity decreased above a critical value of developed  
346 surface area (section 3.2) in the same conditions. From a chemical engineer viewpoint, it  
347 could be helpful to estimate the proportion of the ultrasonic power supplied to the reactor that  
348 is assumed to be devoted to chemical effect. So, calibration experiments were made without  
349 glass beads: the ultrasonic power and the triiodide formation rate were both measured for  
350 several electrical power inputs. The obtained data enables to link  $r(\text{I}_3^-)_0$  and  $P_{US}$  for the  
351 different ultrasound frequencies Fig.10.



352  
353 **Fig. 10.**  $I_3^-$  formation rate as a function of calorimetric ultrasonic power for the same electric power  
354 in homogeneous medium ( $0 \text{ g.L}^{-1}$ ,  $V = 500 \text{ mL}$ ,  $T = 20 \pm 1 \text{ }^\circ\text{C}$ )

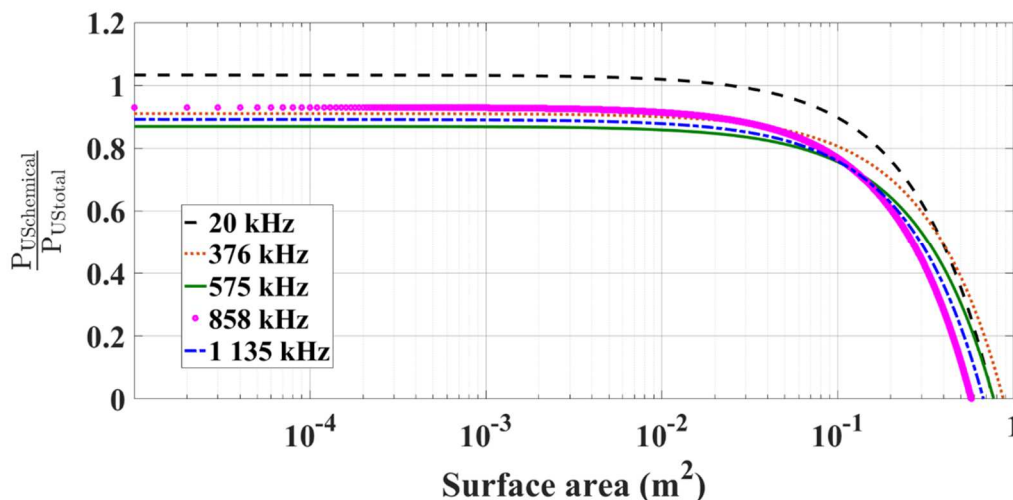
355 For all the frequencies, it can be noted the triiodine formation rate increases with the  
356 ultrasonic power once the cavitation threshold is overpassed [50]. Above this threshold, the  
357 observed increase of the sonochemical activity can be attributed to the growing of acoustic  
358 bubbles population [51]. It was therefore assumed that without particles the ultrasonic power  
359 measured by calorimetry is partly turned into sonochemical activity due to the relationship  
360 between these both ~~parameters~~ variables as suggested by results in **Fig. 10**. Then the linear  
361 approximations of these curves were used as calibration curves (**Fig. 11**) to estimate the  
362 proportion of the equivalent ultrasonic power devoted to chemical activity under  
363 heterogeneous conditions, denoted  $P_{US\text{-chemical}}$ . Even if such an assessment tool may be  
364 ~~criticisable~~ questionable, it can be regarded as a useful tool for preliminary diagnosis tests for  
365 ultrasonic reactors performances.



366  
367 **Fig. 11.** Instance of calibration ( $f = 575 \text{ kHz}$ ,  $0 \text{ g.L}^{-1}$ ,  $V = 500 \text{ mL}$ ,  $T = 20 \pm 1 \text{ }^\circ\text{C}$ ) to estimate the equivalent ultrasonic  
368 power devoted to chemical activity under heterogeneous conditions.  
369

370 This procedure was then extended to all our experimental results under heterogeneous  
371 conditions. It was thereby possible to estimate a power fraction defined as the equivalent

372 ultrasonic power devoted to cavitation sonochemical activity divided by the total ultrasonic  
 373 power estimated by calorimetry. This methodology leads to curves given in **Fig. 12** where the  
 374 power fraction is given as a function of the developed surface area by solid particles within  
 375 the reactor.



376  
 377 **Fig. 12.** Dependence of the ultrasonic power devoted to the sonochemical activity on the developed surface area.

378 Finally, as exhibited in **Fig. 12**, the power fraction remains constant at first, but decreases  
 379 sharply after a critical developed surface area. Therefore, the ultrasonic power distribution  
 380 changes: mainly devoted to sonochemistry for low developed surface areas (below 10<sup>-2</sup> m<sup>2</sup>) it  
 381 is dissipated into mechanical effects for higher areas. So, using this type of diagram can be  
 382 helpful to determine the predominant effect of ultrasound in an heterogeneous medium  
 383 simulated by glass beads and thereby to determine the efficiency of our sonochemical reactor.

384

### 385 **3.4 Acoustic radiation power**

386 In order to estimate directly the sonochemical activity from physical tests, special attention  
 387 has been given to the radiation power, because the calorimetric ultrasonic power seems not to  
 388 be adapted for the entire range of studied developed surface areas (sections 3.1 and 3.2).

389 At 575 kHz, acoustic radiation power and calorimetric power were compared for  
 390 homogeneous medium. The obtained values ( $P_{US} = 51.5 \pm 0.5$  W and  $P_{US-rad} = 51.0 \pm 1.0$  W)  
 391 proves our analytical method is efficient. Then the acoustic radiation power was measured at  
 392 575 kHz in the presence of 8-12  $\mu$ m glass beads, at different concentrations, for the same  
 393 calorimetric power ( $P_{US} = 51.5 \pm 0.5$  W). Normalized results of triiodine formation rate,  
 394 calorimetric power and radiation power were compared (**Fig. 13**).

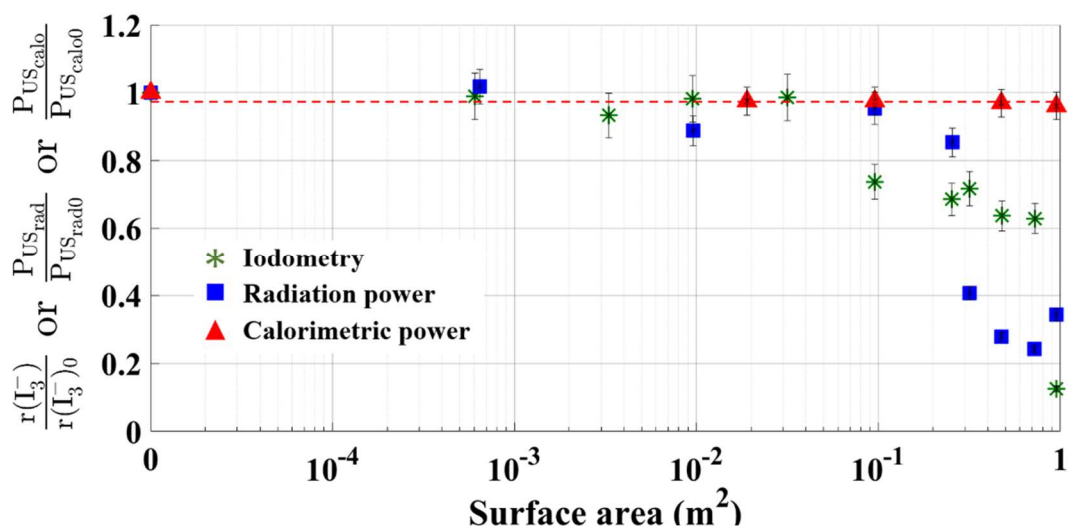


Fig. 13. Comparison of triiodide formation rate, calorimetric power and radiation power in heterogeneous medium ( $d_p = 8-12 \mu\text{m}$ ,  $f = 575 \text{ kHz}$ ,  $V = 500 \text{ mL}$ ,  $T = 20 \pm 1 \text{ }^\circ\text{C}$ )

395  
396  
397

398 The calorimetric power remains constant as mentioned previously (section 3.1), but the  
399 acoustic radiation power appears to follow the same trend as the sonochemical activity  
400 measured via the triiodide formation rate. At low developed surface area, the radiation power  
401 remains constant (ratio close to 1), so the presence of particles does not perturb ultrasound  
402 waves propagation. Nevertheless, above a critical value of developed surface area (around  $10^{-1}$   
403  $\text{m}^2$ ), radiation power decreases drastically. This is due to wave-matter interactions, mainly  
404 scattering and attenuation, induced by glass beads [44-45, 52]. Hence glass beads, whose  
405 acoustic impedance is different than water acoustic impedance, disturb wave propagation  
406 towards the target. As a conclusion, at the studied frequency, contrary to the calorimetric  
407 power, the acoustic radiation power is a relevant parameter to describe the influence of solids  
408 on sonochemical activity.

409

#### 410 4. Conclusions

411 The aim of this paper was to acquire a better knowledge on to study the sonochemical activity  
412 in heterogeneous medium, according to the varying concentration (0-80  $\text{g}\cdot\text{L}^{-1}$ ) and diameter  
413 (8-12 to 6000  $\mu\text{m}$ ) of chemically inert glass beads. A wide range of ultrasonic frequency (20  
414 to 1135 kHz) was used. The ultrasonic power was measured by calorimetry or by radiation,  
415 and the sonochemical activity was monitored by iodide oxidation following the formation rate  
416 of triiodide.

417 Whatever the concentration and diameter of glass beads are, the ultrasonic power measured  
418 by calorimetry was not affected by particles glass beads addition, even when the power supply  
419 was reduced. One might here consider that such a result could be expected since the ultrasonic  
420 power measured by calorimetry only gives general information on the overall energy  
421 available in the system without any distinction on its nature. However, the results from the  
422 chemical characterization have shown dependence between the area of the surface developed  
423 by the particles and the chemical activity of ultrasound. On the contrary, the chemical  
424 characterization has shown dependence between the surface area of the surface developed by



425 the particles and the chemical activity of ultrasound. Indeed, the sonochemical activity  
426 remains constant below a ~~surface area threshold~~ ~~critical area value~~ and it sharply decreases  
427 above it. In our case, it seems the addition of particles did not increase bubbles population by  
428 playing the role of nucleation sites. Above the critical ~~surface~~ area, the activity decrease is due  
429 to wave scattering and attenuation on the one hand, and bubble stabilization on the other hand,  
430 which reduced the energy release.

431 ~~Glass beads~~ addition has the same effect on the sonochemical activity and on the acoustic  
432 radiation power, while the measured calorimetry is unchanged. As a consequence, the  
433 acoustic radiation power is a relevant parameter to describe the influence of solids on  
434 sonochemical activity.

435 The criterion suggested by our results is the ~~surface area developed by~~ of the particles within  
436 the reactor, whose advantage is to take into account both size and concentration of the  
437 heterogeneous media. Once a threshold of the ~~developed surface~~ area is overpassed, a switch  
438 in the proportion of mechanical and chemical energy leads to a decrease of the sonochemical  
439 activity.

## 440 **References**

- 441 [1] K. Muthoosamy, S. Manickam, State of the art and recent advances in the ultrasound-  
442 assisted synthesis, exfoliation and functionalization of graphene derivatives, *Ultrason.*  
443 *Sonochem.* 39 (2017) 478–493. doi:10.1016/j.ultsonch.2017.05.019.
- 444 [2] T. Harifi, M. Montazer, A review on textile sonoprocessing: A special focus on  
445 sonosynthesis of nanomaterials on textile substrates, *Ultrason. Sonochem.* 23 (2015) 1–  
446 10. doi:10.1016/j.ultsonch.2014.08.022.
- 447 [3] K. Vilku, R. Mawson, L. Simons, D. Bates, Applications and opportunities for  
448 ultrasound assisted extraction in the food industry — A review, *Innov. Food Sci. Emerg.*  
449 *Technol.* 9 (2008) 161–169. doi:10.1016/j.ifset.2007.04.014.
- 450 [4] M. Breitbach, D. Bathen, Influence of ultrasound on adsorption processes, *Ultrason.*  
451 *Sonochem.* 8 (2001) 277–283. doi:10.1016/S1350-4177(01)00089-X.
- 452 [5] H. Kim, K. Suslick, The Effects of Ultrasound on Crystals: Sonocrystallization and  
453 Sonofragmentation, *Crystals.* 8 (2018) 280.1–20. doi:10.3390/cryst8070280.
- 454 [6] A. Keck, E. Gilbert, R. Köster, Influence of particles on sonochemical reactions in  
455 aqueous solutions, *Ultrasonics.* 40 (2002) 661–665. doi:10.1016/S0041-624X(02)00195-  
456 6.
- 457 [7] T. Tuziuti, K. Yasui, M. Sivakumar, Y. Iida, N. Miyoshi, Correlation between Acoustic  
458 Cavitation Noise and Yield Enhancement of Sonochemical Reaction by Particle  
459 Addition, *J. Phys. Chem. A.* 109 (2005) 4869–4872. doi:10.1021/jp0503516.
- 460 [8] N. Her, J.-S. Park, Y. Yoon, Sonochemical enhancement of hydrogen peroxide  
461 production by inert glass beads and TiO<sub>2</sub>-coated glass beads in water, *Chem. Eng. J.* 166  
462 (2011) 184–190. doi:10.1016/j.cej.2010.10.059.
- 463 [9] D. Stoian, N. Eshtiaghi, J. Wu, R. Parthasarathy, Intensification of sonochemical  
464 reactions in solid-liquid systems under fully suspended condition, *Chem. Eng. Process.*  
465 *Process Intensif.* 123 (2018) 34–44. doi:10.1016/j.cep.2017.10.025.
- 466 [10] Y. Son, D. Lee, W. Lee, J. Park, W. H. Lee, M. Ashokkumar, Cavitation activity in  
467 heterogeneous systems containing fine particles, *Ultrason. Sonochem.* 58 (2019) 104599.  
468 doi: 10.1016/j.ultsonch.2019.05.016.

- 469 [11] Y. Lu, N. Riyanto, L.K. Weavers, Sonolysis of synthetic sediment particles: particle  
470 characteristics affecting particle dissolution and size reduction, *Ultrason. Sonochem.* 9  
471 (2002) 181–188. doi:10.1016/S1350-4177(02)00076-7.
- 472 [12] M. Lim, M. Ashokkumar, Y. Son, The effects of liquid height/volume, initial  
473 concentration of reactant and acoustic power on sonochemical oxidation, *Ultrason.*  
474 *Sonochem.* 21 (2014) 1988–1993. doi:10.1016/j.ultsonch.2014.03.005.
- 475 [13] P.R. Gogate, V.S. Sutkar, A.B. Pandit, Sonochemical reactors: Important design and  
476 scale up considerations with a special emphasis on heterogeneous systems, *Chem. Eng.*  
477 *J.* 166 (2011) 1066–1082. doi:10.1016/j.cej.2010.11.069.
- 478 [14] A. Brotchie, F. Grieser, M. Ashokkumar, Effect of Power and Frequency on Bubble-Size  
479 Distributions in Acoustic Cavitation, *Phys. Rev. Lett.* 102 (2009).  
480 doi:10.1103/PhysRevLett.102.084302.
- 481 [15] M. Minnaert, On musical air-bubbles and the sounds of running water, *The London,*  
482 *Edinburgh, and Dublin Philosophical Magazine and Journal of Science.* 16 (1933) 235–  
483 248. doi:10.1080/14786443309462277.
- 484 [16] P. Boldo, C. Pétrier and N. Gondrexon, New Operating Method Improves Calorimetric  
485 Measurement of Ultrasonic Power. Proc. 9th Meeting of the European Society of  
486 Sonochemistry. Badajoz, Spain. pp.147–148.
- 487 [17] Y. Iida, K. Yasui, T. Tuziuti, M. Sivakumar, Sonochemistry and its dosimetry,  
488 *Microchem. J.* 80 (2005) 159–164. doi:10.1016/j.microc.2004.07.016.
- 489 [18] S. Koda, T. Kimura, T. Kondo, H. Mitome, A standard method to calibrate sonochemical  
490 efficiency of an individual reaction system, *Ultrason. Sonochem.* 10 (2003) 149–156.  
491 doi:10.1016/S1350-4177(03)00084-1.
- 492 [19] S. Merouani, O. Hamdaoui, F. Saoudi, M. Chiha, Influence of experimental parameters  
493 on sonochemistry dosimetries: KI oxidation, Fricke reaction and H<sub>2</sub>O<sub>2</sub> production,  
494 *Journal of Hazardous Materials.* 178 (2010) 1007–1014.  
495 doi:10.1016/j.jhazmat.2010.02.039.
- 496 [20] J. Zieniuk, R.C. Chivers, Measurement of ultrasonic exposure with radiation force and  
497 thermal methods, *Ultrasonics.* 14 (1976) 161–172. doi:10.1016/0041-624X(76)90048-2.
- 498 [21] IEC 61161 norm Ultrasonics - Power measurement - Radiation force balances and  
499 performance requirements, 2013.
- 500 [22] R.T. Hekkenberg, K. Beissner, B. Zeqiri, R.A. Bezemer, M. Hodnett, Validated  
501 ultrasonic power measurements up to 20 W, *Ultrasound Med. Biol.* 27(3) (2001) 427-  
502 438. [https://doi.org/10.1016/S0301-5629\(00\)00344-6](https://doi.org/10.1016/S0301-5629(00)00344-6).
- 503 [23] B. Zeqiri, L. Wang, P. Miloro, S.P. Robinson, A radiation force balance target material  
504 for applications below 0.5 MHz, *Ultrasound Med. Biol.* 46(9) (2020) 2520–2529.  
505 <https://doi.org/10.1016/j.ultrasmedbio.2020.04.031>.
- 506 [24] T. Kikuchi, T. Uchida, Calorimetric method for measuring high ultrasonic power using  
507 water as a heating material, *J. Phys.: Conf. Ser.* 279 (2011) 012012. doi:10.1088/1742-  
508 6596/279/1/012012.
- 509 [25] T. Uchida, T. Kikuchi, Effect of Heat Generation of Ultrasound Transducer on  
510 Ultrasonic Power Measured by Calorimetric Method, *Jpn. J. Appl. Phys.* 52 (2013)  
511 07HC01. doi:10.7567/JJAP.52.07HC01.
- 512 [26] G. Morgado, S. Miqueleti, R.P.B. Costa-Felix, Measurement of ultrasound power using  
513 a calorimeter, *J. Phys.: Conf. Ser.* 975 (2018) 012010. doi.org/10.1088/1742-  
514 6596/975/1/012010.
- 515 [27] G.J. Price, E.J. Lenz, The use of dosimeters to measure radical production in aqueous  
516 sonochemical systems, *Ultrasonics.* 31 (1993) 451–456. doi:10.1016/0041-  
517 624X(93)90055-5.

- 518 [28] C. Petrier, A. Jeunet, J.L. Luche, G. Reverdy, Unexpected frequency effects on the rate  
519 of oxidative processes induced by ultrasound, *J. Am. Chem. Soc.* 114 (1992) 3148–  
520 3150. doi:10.1021/ja00034a077.
- 521 [29] P. Kanthale, M. Ashokkumar, F. Grieser, Sonoluminescence, sonochemistry (H<sub>2</sub>O<sub>2</sub>  
522 yield) and bubble dynamics: Frequency and power effects, *Ultrason. Sonochem.* 15  
523 (2008) 143–150. doi:10.1016/j.ultsonch.2007.03.003.
- 524 [30] R.J. Wood, J. Lee, M.J. Bussemaker, A parametric review of sonochemistry: Control  
525 and augmentation of sonochemical activity in aqueous solutions, *Ultrason. Sonochem.*  
526 38 (2017) 351–370. doi:10.1016/j.ultsonch.2017.03.030.
- 527 [31] S. Merouani, H. Ferkous, O. Hamdaoui, Y. Rezgui, M. Guemini, A method for  
528 predicting the number of active bubbles in sonochemical reactors, *Ultrason. Sonochem.*  
529 22 (2015) 51–58. doi:10.1016/j.ultsonch.2014.07.015.
- 530 [32] K.S. Suslick, S.J. Doktycz, E.B. Flint, On the origin of sonoluminescence and  
531 sonochemistry, *Ultrasonics*. 28 (1990) 280–290. doi:10.1016/0041-624X(90)90033-K.
- 532 [33] H. Mitome, Action of Ultrasound on Particles and Cavitation Bubbles, WCU 2003, Paris  
533 (2003) 1231-1235.
- 534 [34] L. Zhang, V. Belova, H. Wang, W. Dong, H. Möhwald, Controlled Cavitation at  
535 Nano/Microparticle Surfaces, *Chem. Mater.* 26 (2014) 2244–2248.  
536 doi:10.1021/cm404194n.
- 537 [35] S. Huang, A. Ihara, H. Watanabe, H. Hashimoto, Effects of Solid Particle Properties on  
538 Cavitation Erosion in Solid-Water Mixtures, *Journal of Fluids Engineering*. 118 (1996)  
539 749–755. doi:10.1115/1.2835505.
- 540 [36] T. Ouerhani, R. Pflieger, W. Ben Messaoud, S.I. Nikitenko, Spectroscopy of  
541 Sonoluminescence and Sonochemistry in Water Saturated with N<sub>2</sub>–Ar Mixtures, *J. Phys.*  
542 *Chem. B*. 119 (2015) 15885–15891. doi:10.1021/acs.jpcc.5b10221.
- 543 [37] G. Mark, A. Tauber, R. Laupert, H.-P. Schuchmann, D. Schulz, A. Mues, C. von  
544 Sonntag, OH-radical formation by ultrasound in aqueous solution – Part II:  
545 Terephthalate and Fricke dosimetry and the influence of various conditions on the  
546 sonolytic yield, *Ultrasonics Sonochemistry*. 5 (1998) 41–52. doi:10.1016/S1350-  
547 4177(98)00012-1.
- 548 [38] E.L. Mead, R.G. Sutherland, R.E. Verrall, The effect of ultrasound on water in the  
549 presence of dissolved gases, *Can. J. Chem.* 54 (1976) 1114–1120. doi:10.1139/v76-159.
- 550 [39] M. A. Beckett, I. Hua, Impact of Ultrasonic Frequency on Aqueous Sonoluminescence  
551 and Sonochemistry, *J. Phys. Chem. A*. 105 (2001) 3796–3802. doi:10.1021/jp003226x.
- 552 [40] R. Kidak, N. H. Ince, Effects of operating parameters on sonochemical decomposition of  
553 phenol, *Journal of Hazardous Materials*. 137 (2006) 1453–1457.  
554 doi:10.1016/j.jhazmat.2006.04.021.
- 555 [41] M. Kitajima, S. Hatanaka, S. Hayashi, Mechanism of O<sub>2</sub>-accelerated sonolysis of  
556 bisphenol A, *Ultrasonics*. 44 (2006) e371–e373. doi:10.1016/j.ultras.2006.05.062.
- 557 [42] R.A. Torres, C. Pétrier, E. Combet, M. Carrier, C. Pulgarin, Ultrasonic cavitation applied  
558 to the treatment of bisphenol A. Effect of sonochemical parameters and analysis of BPA  
559 by-products, *Ultrasonics Sonochemistry*. 15 (2008) 605–611.  
560 doi:10.1016/j.ultsonch.2007.07.003.
- 561 [43] O. Supponen, D. Obreschkow, P. Kobel, M. Farhat, Luminescence from cavitation  
562 bubbles deformed in uniform pressure gradients, *Phys. Rev. E*. 96 (2017) 033114.  
563 doi:10.1103/PhysRevE.96.033114.
- 564 [44] J.R. Allegra, S.A. Hawley, Attenuation of Sound in Suspensions and Emulsions: Theory  
565 and Experiments, *The Journal of the Acoustical Society of America*. 51 (1972) 1545–  
566 1564. doi:10.1121/1.1912999.

- 567 [45] M. Su, M. Xue, X. Cai, Z. Shang, F. Xu, Particle size characterization by ultrasonic  
568 attenuation spectra, *Particuology*. 6 (2008) 276–281. doi:10.1016/j.partic.2008.02.001.
- 569 [46] I. Hua, M.R. Hoffmann, Optimization of ultrasonic irradiation as an advanced oxidation  
570 technology, *Environmental Science & Technology*. 31 (1997) 2237–2243.
- 571 [47] D.G. Wayment, D.J. Casadonte, Frequency effect on the sonochemical remediation of  
572 alachlor, *Ultrasonics Sonochemistry*. 9 (2002) 251–257. [https://doi.org/10.1016/S1350-4177\(02\)00081-0](https://doi.org/10.1016/S1350-4177(02)00081-0).
- 574 [48] F. Guzman-Duque, C. Pétrier, C. Pulgarin, G. Peñuela, R.A. Torres-Palma, Effects of  
575 sonochemical parameters and inorganic ions during the sonochemical degradation of  
576 crystal violet in water, *Ultrasonics Sonochemistry*. 18 (2011) 440–446.  
577 <https://doi.org/10.1016/j.ultsonch.2010.07.019>.
- 578 [49] Y. Gao, N. Gao, Y. Deng, J. Gu, Y. Gu, D. Zhang, Factors affecting sonolytic  
579 degradation of sulfamethazine in water, *Ultrasonics Sonochemistry*. 20 (2013) 1401–  
580 1407. <https://doi.org/10.1016/j.ultsonch.2013.04.007>.
- 581 [50] W. Connolly, F.E. Fox, Ultrasonic Cavitation Thresholds in Water, *J. Acoust. Soc. Am.*  
582 26 (1954) 843–848. doi:10.1121/1.1907427.
- 583 [51] P.R. Gogate, S. Shaha, L. Csoka, Intensification of cavitation activity in the  
584 sonochemical reactors using gaseous additives, *Chem. Eng. J.* 239 (2014) 364–372.  
585 doi:10.1016/j.cej.2013.11.004.
- 586 [52] R.E. Challis, V.J. Pinfield, Ultrasonic wave propagation in concentrated slurries – The  
587 modelling problem, *Ultrasonics*. 54 (2014) 1737–1744. doi:10.1016/j.ultras.2014.04.003.
- 588